BIOPHYSICS

Do photosynthetic complexes use quantum coherence to increase their efficiency? Probably not

Elinor Zerah Harush[1,2] and Yonatan Dubi[1,2]*

Answering the titular question has become a central motivation in the field of quantum biology, ever since the idea was raised following a series of experiments demonstrating wave-like behavior in photosynthetic complexes. Here, we report a direct evaluation of the effect of quantum coherence on the efficiency of three natural complexes. An open quantum systems approach allows us to simultaneously identify their level of "quantumness" and efficiency, under natural physiological conditions. We show that these systems reside in a mixed quantum-classical regime, characterized by dephasing-assisted transport. Yet, we find that the change in efficiency at this regime is minute at best, implying that the presence of quantum coherence does not play a substantial role in enhancing efficiency. However, in this regime, efficiency is independent of any structural parameters, suggesting that evolution may have driven natural complexes to their parameter regime to "design" their structure for other uses.

INTRODUCTION

In the photosynthetic process, energy is transferred from an antenna (where light is collected) to a reaction center (where the energy is converted to chemical energy, to be used later by the organism). Excitons—bound electron–hole pairs—are the energy carriers in the photosynthetic process, carrying the harvested solar energy from the antenna to the reaction center, through a network of bacteriochlorophylls (BChls), the so-called exciton-transfer complex (ETC) (*1*). Interest in the dynamics of excitons in the ETC exploded over the past decade, following recent experiments, where ultrafast nonlinear spectroscopy signals showed long-lived oscillations (*2*–*8*). The discovery of coherent oscillations in ETCs pushed forward the hypothesis that in natural photosynthetic complexes, which are extremely efficient, quantum coherence in the presence of an environment is used to assist energy transfer, an idea that has generated much excitement (and debate) (*9*–*19*).

The problem can basically be summarized in two seemingly simple questions: (i) Can quantum coherence exist during the biologic process of photosynthetic energy transfer? (ii) If it does, is it used in some way by the natural system to enhance its efficiency? The latter question is actually more subtle and perhaps better phrased as (see Fig. 1A): Does the presence of quantum coherence add any functional advantage, such that it played a role in the driving forces that led, through evolution, to the current design of the natural photosynthetic apparatus?

Many theoretical (and experimental) works have addressed these questions, yet the question in the title remains largely unanswered. One reason is that while experiments are performed in vitro with coherent (pulsed) light, natural systems operate under very different conditions, namely, continuous incoherent excitation (*18*, *20*–*24*), and observing coherence under natural conditions is a very challenging task. That and more, it is hard to make the connection between the observed experimental findings and the energy transfer efficiency, which is related to the total rate at which energy can flow from the antenna to the reaction center (two ingredients that are essentially absent in the experiments).

Here, we address the aforementioned questions, using tools developed from the theory of open quantum systems. Our approach allows us to directly evaluate efficiency while taking relevant physical parameters into account and provides a simple way to estimate whether the system is "quantum" or "classical," i.e., to evaluate whether environment-induced dephasing has pushed the system into the classical regime. We find that the answers to the questions posed above are "yes" and "no," namely, that the excitonic system is indeed in the quantum-coherent regime [even for fast dephasing of ~100 fs (*25*)], but that quantum coherence has only a minute effect on transport efficiency. Put simply, our findings suggest that the answer to the question posed in the title is negative.

METHODS

The approach that we take enables us to simultaneously calculate both the total exciton current through the ETC and the exciton population at each BChl site, under the condition of continuous incoherent excitations (*23*, *24*), with physiologically relevant parameters. The joint evaluation of both currents and populations allows us to answer the questions posed in the introduction. First, the exciton current is a direct measure of the ETC efficiency. This is easy to understand; the efficiency is simply the ratio between power output and power input. The power input is constant, and the power output is essentially the exciton energy times the exciton current.

Second, the populations allow us to evaluate the level of "quantumness" of the system. This was recognized in recent work (*26*), where a connection between exciton population, dephasing rate, and the approach to classicality was established, through the mechanism of environment-assisted quantum transport (ENAQT). When an environment acts on a disordered quantum network (such as the ETC), it induces a finite dephasing time. ENAQT is the situation where the dependence of quantum transport on the dephasing rate is nonmonotonic, showing a maximum at some optimal dephasing rate, and was considered to be a possible mechanism for the high efficiency of photosynthetic complexes (*27*, *27*–*42*). The relation between ENAQT and particle populations is as follows. At the quantum regime (very small dephasing rate), the populations are essentially determined by the Hamiltonian structure of the network and the positions of the source and the drain (antenna and reaction center

[1]Department of Chemistry, Ben-Gurion University of the Negev, Beer-Sheva 84105, Israel. [2]Ilse-Katz Institute for Nanoscale Science and Technology, Ben-Gurion University of the Negev, Beer-Sheva 84105, Israel.
*Corresponding author. Email: jdubi@bgu.ac.il

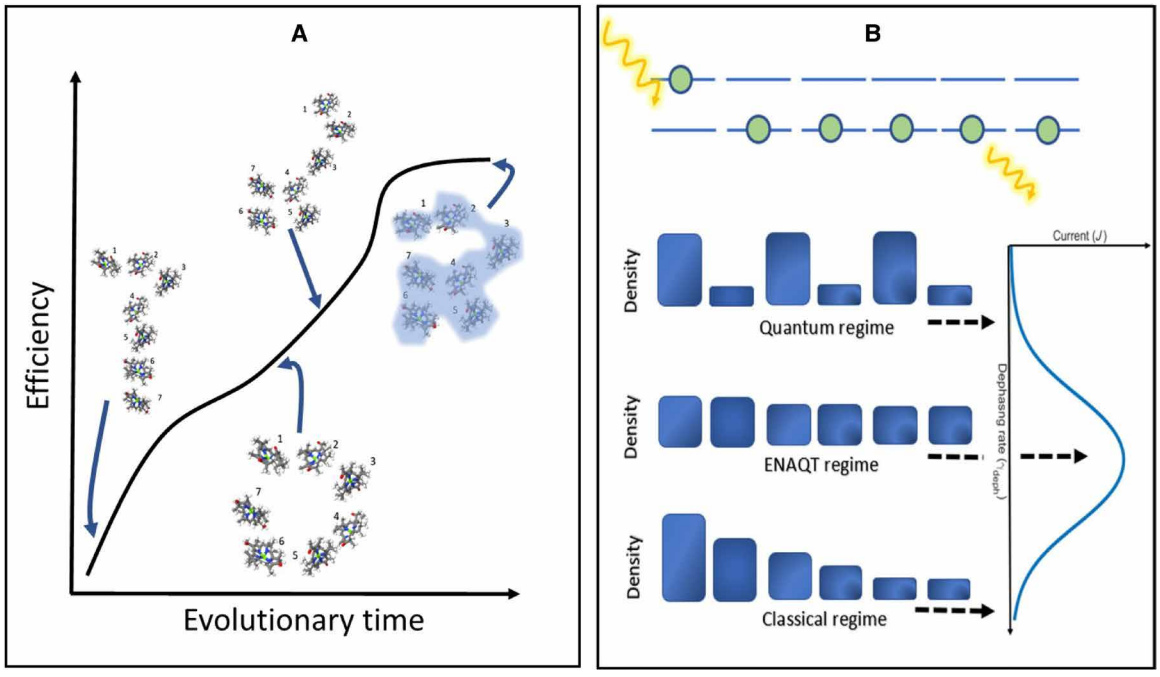

Fig. 1. Mechanisms of efficiency-driven evolution and environment-assisted quantum transport. (**A**) Schematic description of the evolutionary progress of photosynthetic complexes toward their current geometry, with efficiency being the evolutionary driving force. As evolution progresses, the structure of the photosynthetic complex evolves toward its current structure [the Fenna-Matthews-Olson (FMO) complex in this example] while increasing efficiency. Whether this is indeed the evolutionary pathway of photosynthetic complexes, and if so, whether quantum coherence is part of the efficiency enhancement is a central question in the field of quantum biology. (**B**) Schematic depiction of the population uniformization mechanism shown for a uniform chain of six sites (blue lines depict the sites in the chain; yellow arrows show the excitation of first site and extraction from fifth site). The density of the sites is described by blue bars for the quantum regime, ENAQT regime, and classical regime, along with a schematic form for the current versus dephasing curves.

in photosynthetic complexes). As dephasing rate increases, it reduces the variations in populations, so-called "population uniformization," flattening the population distribution, and resulting in an increase in current, which reaches a maximum at some optimal rate. For high dephasing rates, the system becomes essentially classical, and the populations are organized according to Fick's law, i.e., the formation of a uniform gradient between the source and the drain. It is this gradient that can be used to define how classical is the system; once the gradient is fully formed (such that increasing the dephasing rate no longer changes the populations), one can say that the system is classical. The population uniformization mechanism is depicted in Fig. 1B.

In what follows, we evaluate both the transfer efficiency and the populations from the Linbdlad quantum master equation (*43*), taking physically relevant parameters (detailed form of the Lindblad equation is given in section S1). The dephasing rate serves as a free parameter in the calculations but can be evaluated from experiments to be in the range of 10 to 10^3 fs. (*2*–*7*).

We consider three different photosynthetic ETCs: the Fenna-Matthews-Olson (FMO) complex, which appears in green sulfur bacteria, the cryptophyte phycocyanin 645 (PC-645) protein, which is a subunit of the photosynthetic apparatus in cryptophyte algae, and light harvesting 2 (LH2), part of the photosynthetic apparatus of the purple photosynthetic bacterium *Rhodopseudomonas acidophila* (their schematic structures are plotted in the insets of Figs. 2, A and B, and 4, respectively). All three complexes were shown to exhibit coherent energy transfer oscillations in nonlinear two-dimensional spectroscopy measurements (*2*, *5*, *6*, *11*, *44*–*47*). The Hamiltonian parametrization of each complex was taken from previous literature (*48*–*52*) and are provided in the Supplementary Materials (section S6). Some crystallographic measurements suggest an updated model of the FMO complex, containing eight BChls instead of seven (*53*, *54*), a structure that has been parametrized and studied in the context of FMO energy transfer [e.g., (*38*, *55*, *56*)]. Here, we chose to focus on the seven BChls model, as previous works demonstrated that the expected difference between the two models would be insignificant (*38*, *56*).

The remaining parameters that are needed to fully define the parameter set are injection and extraction rates, i.e., the rate at which excitons are pushed into the ETC and extracted to the reaction center. The extraction rate can be estimated by considering the time scales of different transport processes that take place in the photosynthetic complexes. For instance, the exciton transfer time between adjacent LH2 complexes was found to be 3 to 100 ps (*3*, *11*, *14*, *18*, *44*, *52*, *57*), and the trapping time of energy by the core complexes in PC-645 was found to be ≈100 ps (*58*). We then set the extraction rate to an average of $\gamma_{ext} = 0.1\ ps^{-1}$. However, a range of extraction rates was tested, and our results and conclusions are essentially insensitive to the extraction rate, as long as it is much larger than the injection rate (see below).

The injection (or excitation) rate is limited by the absorption cross section, which was estimated for by evaluating that there are $\sigma \sim 14$/s (14 excitons/s) for biological intensity of $I \sim 18\frac{W}{m^2}$ (*59*). The sunlight intensity can be as high as $I_{max} \sim 1300\frac{W}{m^2}$ (on a bright day at the equator), which can be absorbed by $N \approx 400$ complexes in one vesicle (*60*, *61*). The resulting upper limit for the injection

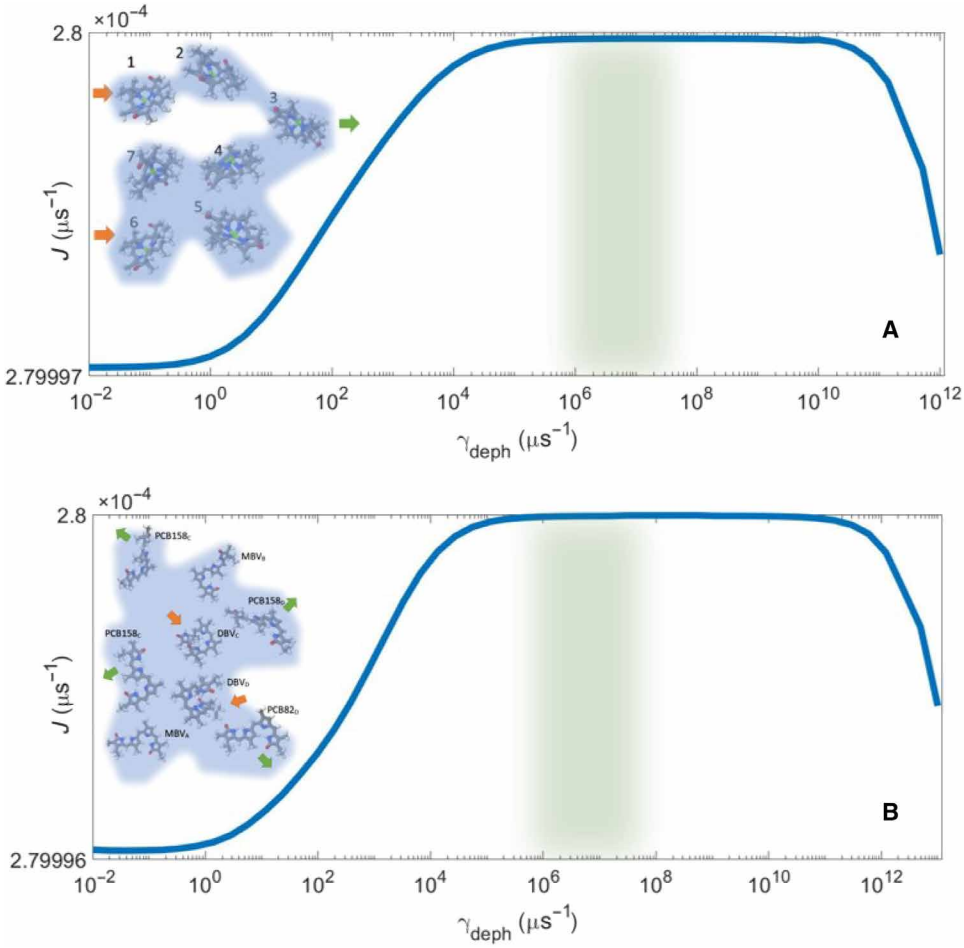

Fig. 2. Effect of environment on photosynthetic transfer efficiency in FMO and PC645. Calculated exciton current as a function of dephasing for the FMO (**A**) and PC-645 (**B**) complexes. The shaded green area indicates the estimated range of physiological dephasing rates. Insets show a schematic description of the exciton complexes (the full Hamiltonians used are provided in section S6).

rate is then $\gamma_{inj} = N \times \sigma \times \frac{I_{max}}{I} \sim 0.4\ \mu s^{-1}$. We note that we have used the same injection rate for all organisms here, although FMO probably does not absorb energy directly from the sun. However, we considered the maximum injection rate that can obtained from the baseplate. This ensures that our results are correct even for extreme conditions (i.e., give an upper bound).

RESULTS

Currents and populations in FMO and PC-645

With all parameters set, one can now evaluate the effect of the environment on the photosynthetic transfer efficiency. In Fig. 2, we plot the exciton current as a function of dephasing rate for the FMO complex (Fig. 2A) and the PC-645 complex (Fig. 2B). Insets are the schematic structures of the complexes, respectively. The similarity between the plots is an indication for the relative insensitivity of the current to the internal structure Hamiltonian (*62*). The green-shaded area in Fig. 2 shows the region of physiological dephasing rates. The ENAQT effect is clearly visible, as the current shows a maximum in the dephasing rate. However, the enhancement in the current due to dephasing is minute, constituting only ~0.0015% increase (even taking extreme values for the injection and extraction rates yields an ENAQT enhancement of only a few percent; see section S3). It seems unlikely that such a small efficiency enhancement would be a meaningful evolutionary driving force; it is more likely that other factors were prominent in the evolutionary design of these photosynthetic complexes.

The structure of the current–dephasing rate dependence already gives a hint that both FMO and PC-645 operate in the ENAQT regime under natural conditions. This can be further corroborated by looking at the exciton populations within the transfer complex for different dephasing rates. As pointed above, the three regimes (quantum, ENAQT, and classical regimes) have very distinct features; the quantum regime is characterized by a spread of the populations determined by the structure of the Hamiltonian, the ENAQT regime by uniform populations, and the classical regime by a linear population gradient from source to drain.

In Fig. 3, the exciton population of the FMO complex is plotted for three values of dephasing rate, corresponding to the quantum ($\gamma_{deph} = 10^{-4}\ \mu s^{-1}$), biological conditions (ENAQT regime, $\gamma_{deph} = 10^{6} \mu s^{-1}$), and classical regime ($\gamma_{deph} = 10^{12}\ \mu s^{-1}$). Figure 3A shows the occupation as a function of site number, but because the FMO is not a simple linear chain, in Fig. 3 (B to D), we show the population on the FMO lattice, color-coded such that the brighter colors represent lower density.

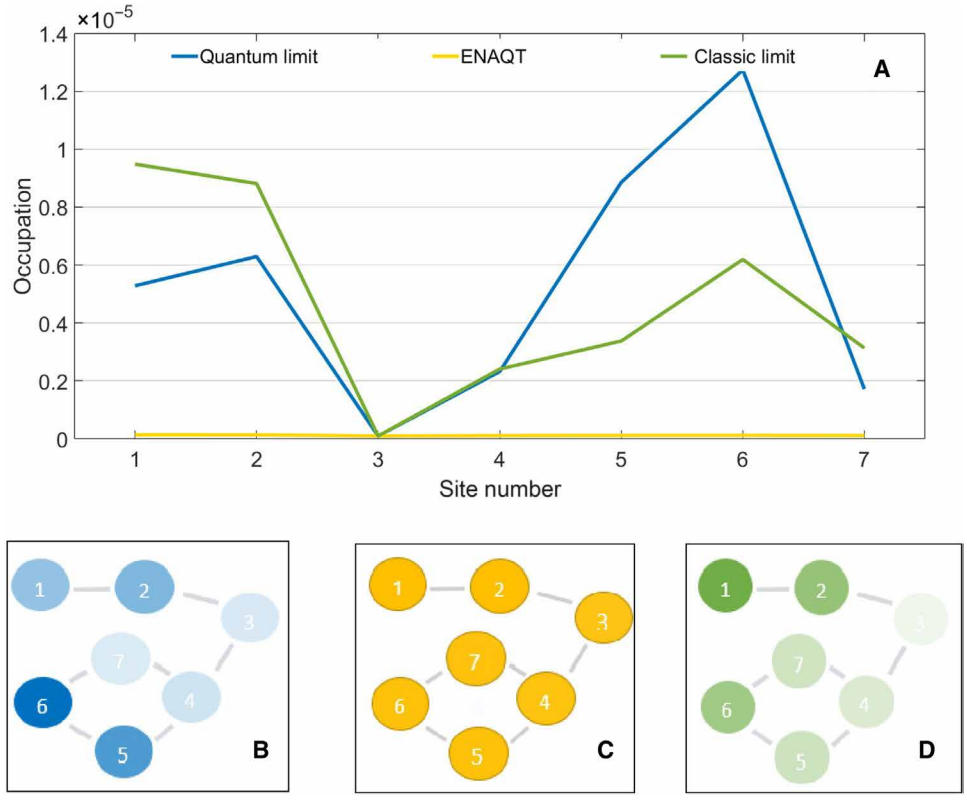

Fig. 3. Exciton density arrangement in the formation of ENAQT. (**A**) Density configuration (i.e., exciton occupation at different sites) of the FMO complex for three different regimes: quantum limit (blue line, $\gamma_{deph} = 10^{-4}\,\mu s^{-1}$), biological condition (yellow line, $\gamma_{deph} = 10^{6}\,\mu s^{-1}$), and classic limit (green line, $\gamma_{deph} = 10^{12}\,\mu s^{-1}$). The transition from the quantum regime toward the classical regime is accompanied by a shift in the density configuration, from a wave function–determined configuration to a uniform gradient between the source and the sink, with a uniform configuration in between (*26*). To more clearly see this, (**B**), (**C**) and (**D**) present the schematic structure of FMO, where each sphere represents a BChl site, and the color brightness reflects its density.

One can clearly observe the population uniformization that leads to ENAQT; in the quantum regime, populations seem disordered and are determined by the interplay between the structure of the wave functions and the source and drain positions. At intermediate dephasing, the population is essentially uniform, and a uniform gradient is formed between source and the drain (sites 6 and 3) for strong dephasing.

ENAQT in LH2

In the LH2 complex, making the connection between ENAQT and population (i.e., recognizing the diffusive regime by observing a population gradient) is harder because there is no simple spatial separation between the antenna (injection sites) and reaction center (source site) such that a gradient can be identified. As depicted in the inset of Fig. 4, the LH2 complex is composed of two rings of BChl pigments, B800 (yellow ring) and B850 (blue ring), named after their energy absorption resonance (in nanometers), connected by a ring of lycopene molecules (gray, long molecules) that absorb energy in the visible region of the spectrum (*50*, *63*–*65*). Each of these parts can absorb light that excites an exciton that later would be transferred from one of the rings to the reaction center (*52*, *57*, *64*). The structure thus enables the occurrence of many exciton transfer paths. Nevertheless, a current versus dephasing curve for LH2 can still reveal the importance (or lack thereof) of coherence in transport.

To evaluate the efficiency of energy transfer in LH2 and its dependence on the dephasing rate, we calculate the excitonic current through LH2, considering multiple paths. Specifically, we assume that an exciton can be excited and extracted in any one of the BChl or molecular sites. In Fig. 4, we plot current as a function of dephasing rate for the LH2 system. Light pink lines are examples of specific paths, and the solid black line is the average curve (green area again marks the regime of physiological dephasing rates). In similarity to the cases of FMO and PC-645, one can see that there is ENAQT, i.e., an increase in the exciton current, and that it is very small, ~0.05%. Similar results are obtained if multiple exciton injections and extractions are considered or if the excitations are of ring eigenstates (see sections S4 and S5).

DISCUSSION

Current, coherence, and classicality

Figures 2 and 4 establish that there is no substantial increase in the exciton current (and hence the efficiency) when comparing the fully quantum case (zero dephasing rate) and the physiological realistic dephasing rates (10^{6} to $10^{8}\mu s^{-1}$). Before discussing the relation between our results and the question in the title, we wish to elaborate further on the notion of quantum versus classical. What makes the system classical? As pointed above, one definition would be the onset of a population gradient, i.e., classical diffusion and Fick's law

(*26*), but this is an operational definition, which ignores the presence of coherences (off-diagonal terms of the density matrix) (*19*). Formally, coherence is necessary for observing current because the current is proportional to (the imaginary part of) the off-diagonal elements of the density matrix, e.g., coherences. Thus, coherences are present also in the classical regime.

What really defines a classical system is not the lack of any coherence but rather the fact that in a classical system, the coherences can be fully determined from the populations, without any additional information required. This implies no "long range" coherence, in the sense that sites that are not connected via hopping matrix elements in the Hamiltonian will have no coherence between them (i.e., no off-diagonal elements connecting them in the density matrix). This distinction between quantum and classical dynamics was quantified in (*9*), where the authors compared the local currents as derived from the off-diagonal density-matrix elements (i.e., quantum flux), $J_{ij}^{Q} = -2t_{ij}\Im(\rho_{ij})$ and from the diagonal elements (classical flux) $J_{ij}^{C} = \kappa_{ij}(\rho_{ii} - \rho_{jj})$ (where t_{ij} is the hopping matrix element between sites i and j, ρ is the density matrix, and κ_{ij} is the classical exciton hopping rate between sites i and j; see the Supplementary Materials for further details). In a classical regime, the two currents would be the same, implying that quantum coherences carry no additional information over the classical dynamics. This is what was found in (*9*) for the FMO complex.

Going back to our results, as can be clearly seen, there is a substantial drop in current when going toward very high dephasing rates. This occurs because in the classical regime, the system becomes diffusive, with a diffusion coefficient that is proportional to $\sim \bar{t}^2/\gamma_{deph}$ ($\bar{t}$ is some typical hopping matrix element) (*66*). The reduction of current with increasing γ_{deph} (but never to zero) is simply due to the decrease in the diffusion coefficient.

One could then argue that the intermediate dephasing rates observed in natural systems hold a substantial advantage over much higher dephasing rates. Because the system is "fully classical" at such high rates but has substantial quantum coherence in the ENAQT regime, one would then argue that quantum effects are very important in determining the efficiency. Put differently, one could say that evolution drove the design of the light-harvesting system (in structural parameters such as geometry and orientation) away from the classical regime to increase its exciton transfer efficiency.

To counter this argument, we note that the drop in current occurs at unrealistically high dephasing rates, which means that the inherent system parameters would have to be tuned (by evolution) in such a way that pushes the system to the classical regime in physiological dephasing times. However, we find that the regime of ENAQT is extremely robust and depends very weakly on the Hamiltonian parameters (this can also be seen by the similarity between the FMO and PC-645 systems) in line with existing literature (*67*–*70*).

This can be understood by analyzing, for instance, the analytical expressions for currents and populations of linear uniform models (see section S2) (*26*). What we find is that the ENAQT regime is confined to the regime of $\gamma_{inj} < \gamma_{deph} < \frac{2\bar{t}^2}{\gamma_{inj}}$, where $\bar{t}$ is some effective or average hopping matrix element (which can be determined from, e.g., the bandwidth of the quantum system) and assuming $\gamma_{inj} \ll \gamma_{ext}$. Because the injection and extraction rates are external parameters, changing the ENAQT regime would require substantial reduction in the hopping matrix elements, but this would reduce the ability of the system to transfer energy. Presumably, this is the reason all three complexes have similar ranges of hopping matrix elements.

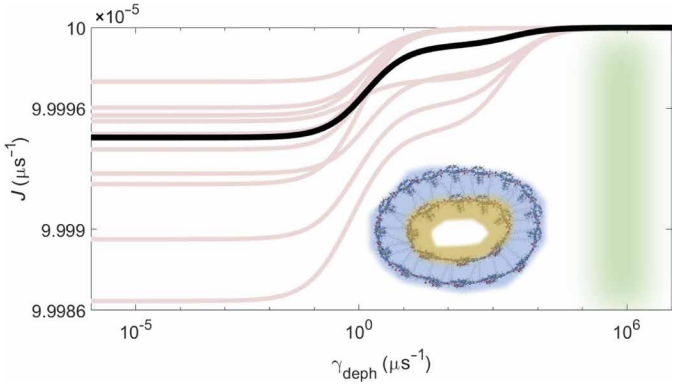

Fig. 4. Effect of environment on photosynthetic transfer efficiency in LH2. Average LH2 exciton current as a function of dephasing rate (black line), calculated for ≈900 possible paths. Pink curves show the current of arbitrary chosen realizations (i.e., entry and exit sites) in LH2. Shaded green area marks the natural dephasing rate. Inset: Schematic description of LH2 transfer network (the full Hamiltonian used is provided in section S6).

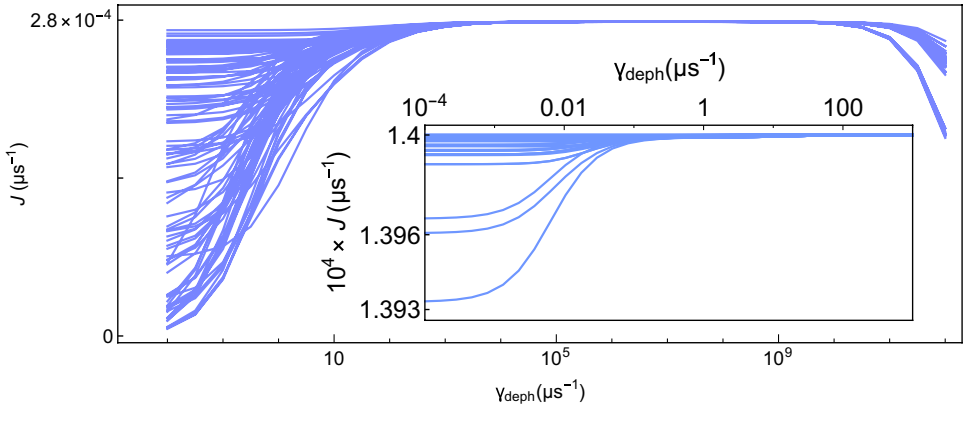

Fig. 5. Current versus dephasing rate for 5000 realizations of FMO-like networks. Energies were kept fixed, while hopping matrix elements were picked from a range of ±200 cm^{-1}. ENAQT is obtained for almost the same range for all realizations, indicating the independence of efficiency in the ENAQT regime (and the regime itself) on the structure of the system.

This analysis implies that the ENAQT regime is really the "natural" regime at which these systems operate; faster dephasing would require dynamics that are much faster than those of the proteins surrounding the ETCs, while longer dephasing times would require lower temperatures or deeper isolation of the chromophores. Figures 1 and 3 demonstrate that, unexpectedly, at the ENAQT regime, the current reaches a maximum that is limited by the injection rate, and is essentially independent of any Hamiltonian parameters.

To directly show this, in Fig. 5, we show the current–dephasing rate curves of more than 5000 random realizations of FMO-like networks. In this calculation, the diagonal elements (which have an absolute value with insignificant contribution to current) and the injection and extraction positions are kept fixed, and the hopping matrix elements, which define the network structure, are distributed randomly in the regime of ±200 cm^{-1}. The currents at the quantum regime differ substantially because they depend on the detailed wave function structure of a given realization (some realizations have very weak coupling between the source and the sink, resulting in small currents at the quantum regime). Similarly, at the classical regime, there is a distribution of currents (because the onset of the classical regime is sensitive to the hopping elements and hence changes between realizations). However, at the ENAQT regime, there is essentially no dependence on the Hamiltonian parameters. This means that no matter how the network is arranged, the current is the same. In other words, at the ENAQT regime, the value of the current is completely indifferent to the network structure. Therefore, an inevitable conclusion is that enhancing the current was not an evolutionary driver to determine the network structure.

This is not unique to the FMO complex. We find similar results for the PC-645 and LH2 complexes (not shown). Moreover, in the ENAQT regime, the system is robust not only against geometrical changes but also to many other parameters. As a specific example (one out of many), we consider the excitation points of LH2. The LH2 complex is coupled not only to external excitations (via direct light absorption) but also to excitation from neighboring complexes. To mimic this effect, in the inset of Fig. 4, we plot the current–dephasing rate curves of the LH2 complex, taking a random number and position of injection and extraction sites (between two and four injection and extraction sites). Clearly, neither the number nor position of the injection sites affects the current in the ENAQT regime.

The picture that emerges from the calculations presented here is as follows. The photosynthetic excitonic transfer networks, despite their structural differences, all operate in an environment with dephasing time τ_{deph} of a few hundred femtoseconds (up to 1 ps), which puts them in the ENAQT regime. This regime is characterized by having an exciton current that is only slightly higher than the fully quantum regime and reaches a maximum that is limited by the injection rate. The real advantage of being in the ENAQT regime is the unexpected essential independence of the current on any particular structural parameters of the system. This leads to the conclusion that the structure of neither FMO, PC-645, nor LH2 did not evolve to enhance efficiency (because it is essentially the same in all of them).

If anything, one could claim that evolution drove the physiological times to be what they are because in this regime, the ETC network structure is irrelevant to efficiency and hence can be used for a different function [stability, for instance (*16*)]. However, one must also consider the possibility that the physiological coherence time was also not part of the evolutionary driving and developed by nothing more than a happy coincidence. The physiological dephasing time seems to be a middle ground; faster coherence is typical to electronic systems but not to vibrational systems, and slower coherence times are unlikely in physiological environment.

Therefore, two central challenges remain for future studies. The first is still to understand what determines the origin of the dephasing time τ_{deph} observed in experiments [e.g., (*71*, *72*)], with the goal of understanding whether the observed values are somehow unique and whether they could be different. The second challenge is to look for other possible evolutionary advantages that the structures of the photosynthetic transfer complexes provide. Overcoming these challenges will push forward the understanding of the possible role of quantum effects in photosynthetic complexes.

SUPPLEMENTARY MATERIALS

Supplementary material for this article is available at http://advances.sciencemag.org/cgi/content/full/7/8/eabc4631/DC1

View/request a protocol for this paper from *Bio-protocol*.

REFERENCES AND NOTES

1. M. Mohseni, Y. Omar, G. S. Engel, M. B. Plenio, *Quantum Effects in Biology* (Cambridge Univ. Press, 2014).
2. H. Lee, Y. Cheng, G. Fleming, Coherence dynamics in photosynthesis: Protein protection of excitonic coherence. *Science* **316**, 1462–1465 (2007).
3. G. S. Engel, T. R. Calhoun, E. L. Read, T.-K. Ahn, T. Manal, Y.-C. Cheng, R. E. Blankenship, G. R. Fleming, Evidence for wavelike energy transfer through quantum coherence in photosynthetic systems. *Nature* **446**, 782–786 (2007).
4. T. R. Calhoun, N. S. Ginsberg, G. S. Schlau-Cohen, Y.-C. Cheng, M. Ballottari, R. Bassi, G. R. Fleming, Quantum coherence enabled determination of the energy landscape in light-harvesting complex II. *J. Phys. Chem. B.* **113**, 16291–16295 (2009).
5. E. Collini, C. Y. Wong, K. E. Wilk, P. M. Curmi, P. Brumer, G. D. Scholes, Coherently wired light-harvesting in photosynthetic marine algae at ambient temperature. *Nature* **463**, 644–647 (2010).
6. G. Panitchayangkoon, D. Hayes, K. A. Fransted, J. R. Caram, E. Harel, J. Wen, R. E. Blankenship, G. S. Engel, Long-lived quantum coherence in photosynthetic complexes at physiological temperature. *Proc. Natl. Acad. Sci. U.S.A.* **107**, 12766–12770 (2010).
7. G. Panitchayangkoon, D. V. Voronine, D. Abramavicius, J. R. Caram, N. H. Lewis, S. Mukamel, G. S. Engel, Direct evidence of quantum transport in photosynthetic light-harvesting complexes. *Proc. Natl. Acad. Sci. U.S.A.* **108**, 20908–20912 (2011).
8. R. E. Blankenship, D. M. Tiede, J. Barber, G. W. Brudvig, G. Fleming, M. Ghirardi, M. Gunner, W. Junge, D. M. Kramer, A. Melis, T. A. Moore, C. C. Moser, D. G. Nocera, A. J. Nozik, D. R. Ort, W. W. Parson, R. C. Prince, R. T. Sayre, Comparing photosynthetic and photovoltaic efficiencies and recognizing the potential for improvement. *Science* **332**, 805–809 (2011).
9. J. Wu, F. Liu, J. Ma, R. J. Silbey, J. Cao, Efficient energy transfer in light-harvesting systems: Quantum-classical comparison, flux network, and robustness analysis. *J. Chem. Phys.* **137**, 174111 (2012).
10. R. D. J. Leon-Montiel, I. Kassal, J. P. Torres, Importance of excitation and trapping conditions in photosynthetic environment-assisted energy transport. *J. Phys. Chem. B.* **118**, 10588–10594 (2014).
11. H. W. Rathbone, J. A. Davis, K. A. Michie, S. C. Goodchild, N. O. Robertson, P. M. Curmi, Coherent phenomena in photosynthetic light harvesting: Part two—Observations in biological systems. *Biophys. Rev.* **10**, 1443–1463 (2018).
12. G. Fleming, S. Huelga, M. Plenio, Focus on quantum effects and noise in biomolecules. *New J. Phys.* **13**, 115002 (2011).
13. I. Kassal, J. Yuen-Zhou, S. Rahimi-Keshari, Does coherence enhance transport in photosynthesis. *J. Phys. Chem. Lett.* **4**, 362–367 (2013).
14. H.-G. Duan, V. I. Prokhorenko, R. J. Cogdell, K. Ashraf, A. L. Stevens, M. Thorwart, R. D. Miller, Nature does not rely on long-lived electronic quantum coherence for photosynthetic energy transfer. *Proc. Natl. Acad. Sci. U.S.A.* **114**, 8493–8498 (2017).
15. A. Chenu, G. D. Scholes, Coherence in energy transfer and photosynthesis. *Annu. Rev. Phys. Chem.* **66**, 69–96 (2015).
16. N. Keren, Y. Paltiel, Photosynthetic energy transfer at the quantum/classical border. *Trends Plant Sci.* **23**, 497–506 (2018).
17. J. Cao, R. J. Cogdell, D. F. Coker, H.-G. Duan, J. Hauer, U. Kleinekathöfer, T. L. Jansen, T. Mančal, R. D. Miller, J. P. Ogilvie, V. I. Prokhorenko, T. Renger, H.-S. Tan, R. Tempelaar,

M. Thorwart, E. Thyrhaug, S. Westenhoff, D. Zigmantas, Quantum biology revisited. *Sci. Adv.* **6**, eaaz4888 (2020).
18. S. Bourne Worster, C. Stross, F. M. Vaughan, N. Linden, F. R. Manby, Structure and efficiency in bacterial photosynthetic light harvesting. *J. Phys. Chem. Lett.* **10**, 7383–7390 (2019).
19. P.-Y. Yang, J. Cao, Steady-state analysis of light-harvesting energy transfer driven by incoherent light: From dimers to networks. *J. Phys. Chem. Lett.* **11**, 7204–7211 (2020).
20. D. Manzano, Correction: Quantum transport in networks and photosynthetic complexes at the steady state. *PLOS ONE* **8**, e57041 (2013).
21. K. M. Pelzer, T. Can, S. K. Gray, D. K. Morr, G. S. Engel, Coherent transport and energy flow patterns in photosynthesis under incoherent excitation. *J. Phys. Chem. B.* **118**, 2693–2702 (2014).
22. L. A. Pachón, J. D. Botero, P. Brumer, Open system perspective on incoherent excitation of light-harvesting systems. *J. Phys. B* **50**, 184003 (2017).
23. P. Brumer, Shedding (incoherent) light on quantum effects in light-induced biological processes. *J. Phys. Chem. Lett.* **9**, 2946–2955 (2018).
24. L. F. Morales-Curiel, R. D. J. León-Montiel, Photochemical dynamics under incoherent illumination: Light harvesting in self-assembled molecular j-aggregates. *J. Chem. Phys.* **152**, 074304 (2020).
25. E. Thyrhaug, R. Tempelaar, M. J. Alcocer, K. Žídek, D. Bína, J. Knoester, T. L. Jansen, D. Zigmantas, Identification and characterization of diverse coherences in the Fenna-Matthews-Olson complex. *Nat. Chem.* **10**, 780–786 (2018).
26. E. Zerah-Harush, Y. Dubi, Universal origin for environment-assisted quantum transport in exciton transfer networks. *J. Phys. Chem. Lett.* **9**, 1689–1695 (2018).
27. F. Caruso, A. W. Chin, A. Datta, S. F. Huelga, M. B. Plenio, Highly efficient energy excitation transfer in light-harvesting complexes: The fundamental role of noise-assisted transport. *J. Chem. Phys.* **131**, 105106 (2009).
28. P. Rebentrost, M. Mohseni, I. Kassal, S. Lloyd, A. Aspuru-Guzik, Environment-assisted quantum transport. *New J. Phys.* **11**, 033003 (2009).
29. M. Mohseni, P. Rebentrost, S. Lloyd, A. Aspuru-Guzik, Environment-assisted quantum walks in photosynthetic energy transfer. *J. Chem. Phys.* **129**, 174106 (2008).
30. A. W. Chin, A. Datta, F. Caruso, S. F. Huelga, M. B. Plenio, Noise-assisted energy transfer in quantum networks and light-harvesting complexes. *New J. Phys.* **12**, 065002 (2010).
31. M. B. Plenio, S. F. Huelga, Dephasing-assisted transport: Quantum networks and biomolecules. *New J. Phys.* **10**, 113019 (2008).
32. I. Kassal, A. Aspuru-Guzik, Environment-assisted quantum transport in ordered systems. *New J. Phys.* **14**, 053041 (2012).
33. F. Caruso, Universally optimal noisy quantum walks on complex networks. *New J. Phys.* **16**, 055015 (2014).
34. Y. Li, F. Caruso, E. Gauger, S. C. Benjamin, "Momentum rejuvenation" underlies the phenomenon of noise-assisted quantum energy flow. *New J. Phys.* **17**, 013057 (2015).
35. A. Marais, I. Sinayskiy, A. Kay, F. Petruccione, A. Ekert, Decoherence-assisted transport in quantum networks. *New J. Phys.* **15**, 013038 (2013).
36. I. Sinayskiy, A. Marais, F. Petruccione, A. Ekert, Decoherence-assisted transport in a dimer system. *Phys. Rev. Lett.* **108**, 020602 (2012).
37. H.-B. Chen, N. Lambert, Y.-C. Cheng, Y.-N. Chen, F. Nori, Using non-markovian measures to evaluate quantum master equations for photosynthesis. *Sci. Rep.* **5**, 12753 (2015).
38. Y. Dubi, Interplay between dephasing and geometry and directed heat flow in exciton transfer complexes. *J. Phys. Chem. C* **119**, 25252–25259 (2015).
39. G. P. Berman, A. I. Nesterov, G. V. Lopez, R. T. Sayre, Superradiance transition and nonphotochemical quenching in photosynthetic complexes. *J. Phys. Chem. C* **119**, 22289–22296 (2015).
40. S. Baghbanzadeh, I. Kassal, Distinguishing the roles of energy funnelling and delocalization in photosynthetic light harvesting. *Phys. Chem. Chem. Phys.* **18**, 7459–7467 (2016).
41. J. Cao, R. J. Silbey, Optimization of exciton trapping in energy transfer processes. *J. Phys. Chem. A* **113**, 13825–13838 (2009).
42. M. Sarovar, A. Ishizaki, G. R. Fleming, K. B. Whaley, Quantum entanglement in photosynthetic light-harvesting complexes. *Nat. Phys.* **6**, 462–467 (2010).
43. H.-P. Breuer, F. Petruccione, *The Theory of Open Quantum Systems* (Oxford Univ. Press on Demand, 2002).
44. R. Hildner, D. Brinks, J. B. Nieder, R. J. Cogdell, N. F. Hulst, Quantum coherent energy transfer over varying pathways in single light-harvesting complexes. *Science* **340**, 1448–1451 (2013).
45. F. Ma, L.-J. Yu, R. Hendrikx, Z.-Y. Wang-Otomo, R. Van Grondelle, Excitonic and vibrational coherence in the excitation relaxation process of two lh1 complexes as revealed by two-dimensional electronic spectroscopy. *J. Phys. Chem. Lett.* **8**, 2751–2756 (2017).
46. M. Ferretti, V. I. Novoderezhkin, E. Romero, R. Augulis, A. Pandit, D. Zigmantas, R. van Grondelle, The nature of coherences in the b820 bacteriochlorophyll dimer revealed by two-dimensional electronic spectroscopy. *Phys. Chem. Chem. Phys.* **16**, 9930–9939 (2014).
47. J. C. Dean, T. Mirkovic, Z. S. Toa, D. G. Oblinsky, G. D. Scholes, Vibronic enhancement of algae light harvesting. *Chem* **1**, 858–872 (2016).
48. M. Cho, H. M. Vaswani, T. Brixner, J. Stenger, G. R. Fleming, Exciton analysis in 2d electronic spectroscopy. *J. Phys. Chem. B.* **109**, 10542–10556 (2005).
49. B. Hein, C. Kreisbeck, T. Kramer, Modelling of oscillations in two-dimensional echo-spectra of the Fenna-Matthews-Olson complex. *New J. Phys.* **14**, 023018 (2012).
50. S. Tretiak, C. Middleton, V. Chernyak, S. Mukamel, Exciton hamiltonian for the bacteriochlorophyll system in the LH2 antenna complex of purple bacteria. *J. Phys. Chem. B* **104**, 4519–4528 (2000).
51. S. Tretiak, C. Middleton, V. Chernyak, S. Mukamel, Bacteriochlorophyll and carotenoid excitonic couplings in the LH2 system of purple bacteria. *J. Phys. Chem. B* **104**, 9540–9553 (2000).
52. T. Mirkovic, A. B. Doust, J. Kim, K. E. Wilk, C. Curutchet, B. Mennucci, R. Cammi, P. M. G. Curmi, G. D. Scholes, Ultrafast light harvesting dynamics in the cryptophyte phycocyanin 645. *Photochem. Photobiol. Sci.* **6**, 964 (2007).
53. A. Ben-Shem, F. Frolow, N. Nelson, Evolution of photosystem I – From symmetry through pseudosymmetry to asymmetry. *FEBS Lett.* **564**, 274–280 (2004).
54. D. E. Tronrud, J. Wen, L. Gay, R. E. Blankenship, The structural basis for the difference in absorbance spectra for the FMO antenna protein from various green sulfur bacteria. *Photosynth. Res.* **100**, 79–87 (2009).
55. G. Ritschel, J. Roden, W. T. Strunz, A. Aspuru-Guzik, A. Eisfeld, Absence of quantum oscillations and dependence on site energies in electronic excitation transfer in the Fenna-Matthews-Olson trimer. *J. Phys. Chem. Lett.* **2**, 2912–2917 (2011).
56. J. Moix, J. Wu, P. Huo, D. Coker, J. Cao, Efficient energy transfer in light-harvesting systems, III: The influence of the eighth bacteriochlorophyll on the dynamics and efficiency in FMO. *J. Phys. Chem. Lett.* **2**, 3045–3052 (2011).
57. S. Hess, M. Chachisvilis, K. Timpmann, M. Jones, G. Fowler, C. Hunter, V. Sundström, Temporally and spectrally resolved subpicosecond energy transfer within the peripheral antenna complex (LH2) and from LH2 to the core antenna complex in photosynthetic purple bacteria. *Proc. Natl. Acad. Sci. U.S.A.* **92**, 12333–12337 (1995).
58. C. D. Van der Weij-De Wit, A. B. Doust, I. H. M. van Stokkum, J. P. Dekker, K. E. Wilk, P. M. G. Curmi, R. van Grondelle, Phycocyanin sensitizes both photosystem I and photosystem II in cryptophyte *chroomonas* CCMP270 cells. *Biophys. J.* **94**, 2423–2433 (2008).
59. T. Geyer, V. Helms, Reconstruction of a kinetic model of the chromatophore vesicles from rhodobacter sphaeroides. *Biophys. J.* **91**, 927–937 (2006).
60. S. Scheuring, J. N. Sturgis, V. Prima, A. Bernadac, D. Lévy, J.-L. Rigaud, Watching the photosynthetic apparatus in native membranes. *Proc. Natl. Acad. Sci. U.S.A.* **101**, 11293–11297 (2004).
61. S. Scheuring, J.-L. Rigaud, J. N. Sturgis, Variable lh2 stoichiometry and core clustering in native membranes of rhodospirillum photometricum. *EMBO J.* **23**, 4127–4133 (2004).
62. M. K. Sener, D. Lu, T. Ritz, S. Park, P. Fromme, K. Schulten, Robustness and optimality of light harvesting in cyanobacterial photosystem I. *J. Phys. Chem. B.* **106**, 7948–7960 (2002).
63. G. McDermott, S. Prince, A. Freer, A. Hawthornthwaite-Lawless, M. Papiz, R. Cogdell, N. Isaacs, Crystal structure of an integral membrane light-harvesting complex from photosynthetic bacteria. *Nature* **374**, 517–521 (1995).
64. N. W. Isaacs, R. J. Cogdell, A. A. Freer, S. M. Prince, Light-harvesting mechanisms in purple photosynthetic bacteria. *Curr. Opin. Struct. Biol.* **5**, 794–797 (1995).
65. J. Koepke, X. Hu, C. Muenke, K. Schulten, H. Michel, The crystal structure of the light-harvesting complex II (b800-850) from rhodospirillum molischianum. *Structure* **4**, 581–597 (1996).
66. J. Dziarmaga, W. H. Zurek, M. Zwolak, Non-local quantum superpositions of topological defects. *Nat. Phys.* **8**, 49–53 (2012).
67. A. Shabani, M. Mohseni, H. Rabitz, S. Lloyd, Numerical evidence for robustness of environment-assisted quantum transport. *Phys. Rev. E* **89**, 042706 (2014).
68. D. Hayes, J. Wen, G. Panitchayangkoon, R. E. Blankenship, G. S. Engel, Robustness of electronic coherence in the Fenna-Matthews-Olson complex to vibronic and structural modifications. *Faraday Discuss.* **150**, 459–469 (2011).
69. L. A. Baker, S. Habershon, Robustness, efficiency, and optimality in the Fenna-Matthews-Olson photosynthetic pigment-protein complex. *J. Chem. Phys.* **143**, 105101 (2015).
70. M. Maiuri, E. E. Ostroumov, R. G. Saer, R. E. Blankenship, G. D. Scholes, Coherent wavepackets in the Fenna-Matthews-Olson complex are robust to excitonic-structure perturbations caused by mutagenesis. *Nat. Chem.* **10**, 177–183 (2018).
71. L. A. Pachón, P. Brumer, Physical basis for long-lived electronic coherence in photosynthetic light-harvesting systems. *J. Phys. Chem. Lett.* **2**, 2728–2732 (2011).
72. Z. Zhang, J. Wang, Origin of long-lived quantum coherence and excitation dynamics in pigment-protein complexes. *Sci. Rep.* **6**, 37629 (2016).

Acknowledgments: E.Z.H. acknowledges support from the Ilse Katz Institute for Nanoscale Science & Technology. We are grateful to M. Zwolak for valuable discussions. **Funding:** This work was supported by the Israel Science Fund grant no. 1360/17. **Author contributions:** E.Z.H. and Y.D. both conceived and performed the research and wrote the paper. **Competing interests:** The authors declare that they have no competing interests. **Data and materials availability:** All data needed to evaluate the conclusions in the paper are present in the paper and/or the Supplementary Materials. Additional data related to this paper may be requested from the authors.

Submitted 26 April 2020
Accepted 31 December 2020
Published 17 February 2021
10.1126/sciadv.abc4631

Citation: E. Zerah Harush, Y. Dubi, Do photosynthetic complexes use quantum coherence to increase their efficiency? Probably not. *Sci. Adv.* **7**, eabc4631 (2021).